

Article

Design, Synthesis, and Photo-Responsive Properties of a Collagen Model Peptide Bearing an Azobenzene

Daisuke Sato ^{1,2,*} , Hitomi Goto ², Yui Ishizaki ², Tetsuya Narimatsu ² and Tamaki Kato ^{2,*}¹ Graduate School of Pharmaceutical Sciences, Kyushu University, Fukuoka 812-8582, Japan² Graduate School of Life Science and Systems Engineering, Kyushu Institute of Technology, Kitakyushu 808-0196, Japan

* Correspondence: sato.daisuke.618@m.kyushu-u.ac.jp (D.S.); tmkato@life.kyutech.ac.jp (T.K.)

Abstract: Collagen is a vital component of the extracellular matrix in animals. Collagen forms a characteristic triple helical structure and plays a key role in supporting connective tissues and cell adhesion. The ability to control the collagen triple helix structure is useful for medical and conformational studies because the physicochemical properties of the collagen rely on its conformation. Although some photo-controllable collagen model peptides (CMPs) have been reported, satisfactory photo-control has not yet been achieved. To achieve this objective, detailed investigation of the isomerization behavior of the azobenzene moiety in CMPs is required. Herein, two CMPs were attached via an azobenzene linker to control collagen triple helix formation by light irradiation. **Azo-(PPG)₁₀** with two (Pro-Pro-Gly)₁₀ CMPs linked via a photo-responsive azobenzene moiety was designed and synthesized. Conformational changes were evaluated by circular dichroism and the *cis-to-trans* isomerization rate calculated from the absorption of the azobenzene moiety indicated that the collagen triple helix structure was partially disrupted by isomerization of the internal azobenzene.

Keywords: peptide; collagen; azobenzene; triple helix; photo-switch; isomerization; photochromic molecule; *cis-trans* isomer



Citation: Sato, D.; Goto, H.; Ishizaki, Y.; Narimatsu, T.; Kato, T. Design, Synthesis, and Photo-Responsive Properties of a Collagen Model Peptide Bearing an Azobenzene. *Organics* **2022**, *3*, 415–429. <https://doi.org/10.3390/org3040027>

Academic Editors: David StC Black and Wim Dehaen

Received: 15 July 2022

Accepted: 17 September 2022

Published: 11 October 2022

Publisher's Note: MDPI stays neutral with regard to jurisdictional claims in published maps and institutional affiliations.



Copyright: © 2022 by the authors. Licensee MDPI, Basel, Switzerland. This article is an open access article distributed under the terms and conditions of the Creative Commons Attribution (CC BY) license (<https://creativecommons.org/licenses/by/4.0/>).

1. Introduction

Collagen is the most abundant protein in mammals, and at least 29 different types of collagen proteins have been identified to date [1]. Collagen is one of the major components of the extracellular matrix in connective tissues, such as ligaments, bones, cartilage, tendons, and skin, and plays a vital role in providing mechanical strength to tissues and regulating cell adhesion and migration [2].

The collagen molecule comprises three polypeptide chains that assemble to form a right-handed triple helical structure [3]. This characteristic three-dimensional structure, the collagen triple helix, is responsible for the physicochemical properties of collagen [4]. The collagen triple helix collapses with warming until the temperature reaches the phase transition temperature (T_m), when the three polypeptide chains that form the three-dimensional structure are dissociated. This denaturation of the collagen molecule leads to a sol-gel transition [5]. The polypeptides in the collagen triple helix have a repetitive primary sequence of Gly- X_{aa} - Y_{aa} , where X_{aa} is usually a proline and Y_{aa} is often a (4R)-hydroxyproline [6]. In this typical sequence, the presence of the smallest amino acid, glycine, every third residue allows the three polypeptide chains to be in close proximity. The 4-Hydroxyproline, abbreviated as Hyp or O, has a greater stabilizing effect on the collagen triple helix compared with proline [7,8].

Collagen has attracted attention in protein conformation and interaction analysis, as a carrier molecule for drug delivery systems, and as a biomaterial for tissue engineering [9–12]. Although collagen is regarded as having high biocompatibility and low immunogenicity, there is a risk that natural collagen derived from animal tissues could

potentially cause an undesired immune response, such as an allergy, and possible contamination with pathogens is also an issue. Therefore, the development of collagen-like peptides that are safer and have more functionality than natural collagen is desirable [13]. Currently, several collagen model peptides (CMPs), including (Pro-Hyp-Gly)₁₀, (Pro-Pro-Gly)₁₀, and other CMPs with similar sequences to these peptides, have been developed to mimic collagen [14].

To use the physicochemical properties of collagen for conformational studies and in biomedical materials, the formation and denaturation of the collagen triple helix need to be controllable in a reversible manner. Light is an ideal external trigger because it is highly selective and harmless when correctly applied [15]. Incorporation of a photo-responsive organic molecule into a CMP can provide a reversible, light-controllable, collagen triple helical structure. Azobenzene is one of the most well-studied photochromic molecules [16–18]. Although the azobenzene molecule usually exists in the *trans*-form, it isomerizes to the *cis*-form upon ultraviolet (UV) irradiation at approximately 350 nm. The conversion from the *cis*- to the *trans*-form can be also achieved using visible (Vis) light irradiation near 450 nm or by a temperature change (i.e., thermal effect) [19]. Because the structure of azobenzene can be easily converted from one form to another by light irradiation at specific wavelengths, azobenzene has been widely used as a photo-switch in biological applications [20–22]. Azobenzene derivatives that can be isomerized by Vis light irradiation, without the use of UV light, have been developed [23–26] with a wide range of applications. Reversible control of the major secondary structural motifs of peptides and proteins, such as helices [27–32] and hairpins [33,34], has been studied using azobenzene. Azobenzene has also been used in the functional regulation of proteins, including receptors [35], enzymes [36], ion channels [37], and motor proteins [38], and also nucleic acids [39].

Light-responsive CMPs bearing an azobenzene molecule on the side chain of the peptide have been reported [40–42]. Although these synthesized collagen peptides were photo responsive, the collagen triple helix structure could be only partially regulated by the light irradiation. Such side chain-modified (i.e., branched) CMPs tend to be relatively complicated to synthesize and it is difficult to alter the peptide sequence. In addition, the azobenzene moiety on the side chain may sterically disturb the formation of the triple helical structure, which results in the original physicochemical properties of the collagen peptide chain not being reproduced in CMPs incorporating azobenzene in this manner. Thus, estimation of the properties of CMPs may be difficult at the molecular design stage. Although azobenzene-terminated CMPs have been also developed [43,44], the structures formed by these short CMPs, which contained at most five of repeats of the POG unit, favored a random coil, over a triple helix, structure because of the *trans*-to-*cis* isomerization of the terminal azobenzene. This disruption was caused by the relatively loose triple helical structure because of the shorter CMP chain. Moreover, current interest in CMPs appears to be directed toward morphological observations and the preparation of various types of three-dimensional nanoarchitectures [45]. Few studies have reported on photo-responsive CMPs incorporating azobenzene in a linearly linked manner and few kinetics studies have investigated the *trans*-to-*cis* isomerization upon UV irradiation or thermal *cis*-to-*trans* isomerization of such peptides.

In the present study, a linear photo-responsive collagen peptide bearing an azobenzene molecule was designed and synthesized and the effect of the photo-isomerization of the azobenzene moiety on the collagen triple helix structure was evaluated (Figure 1a). A kinetic assay of the thermal *cis*-to-*trans* isomerization of the azobenzene moiety of the CMPs was also performed to investigate the isomerization when azobenzene was conjugated to the CMPs. The 4,4'-Diaminoazobenzene was used as the azobenzene moiety, and the collagen peptide (Pro-Pro-Gly)₁₀, which is the simplest CMP, was conjugated at both ends of the azobenzene moiety via glycine linkers. The 9-Fluorenylmethoxycarbonyl (Fmoc) groups on the N^α-termini of the CMPs were retained to provide the potential for further modification by terminal functionalization. The glycine linker was expected to act as a buffer to alleviate the steric strain caused by the linking via the azobenzene during collagen

triple helix formation. **Azo-(PPG)₁₀** should form a collagen triple helix structure and this conformation was expected to be disrupted by the isomerization of the internal azobenzene moiety induced by UV-Vis light irradiation or a thermal effect (Figure 1b). The disassembled CMP chains should re-aggregate to form the helix again on cooling, which means that this conformational change in the CMPs should be reversible.

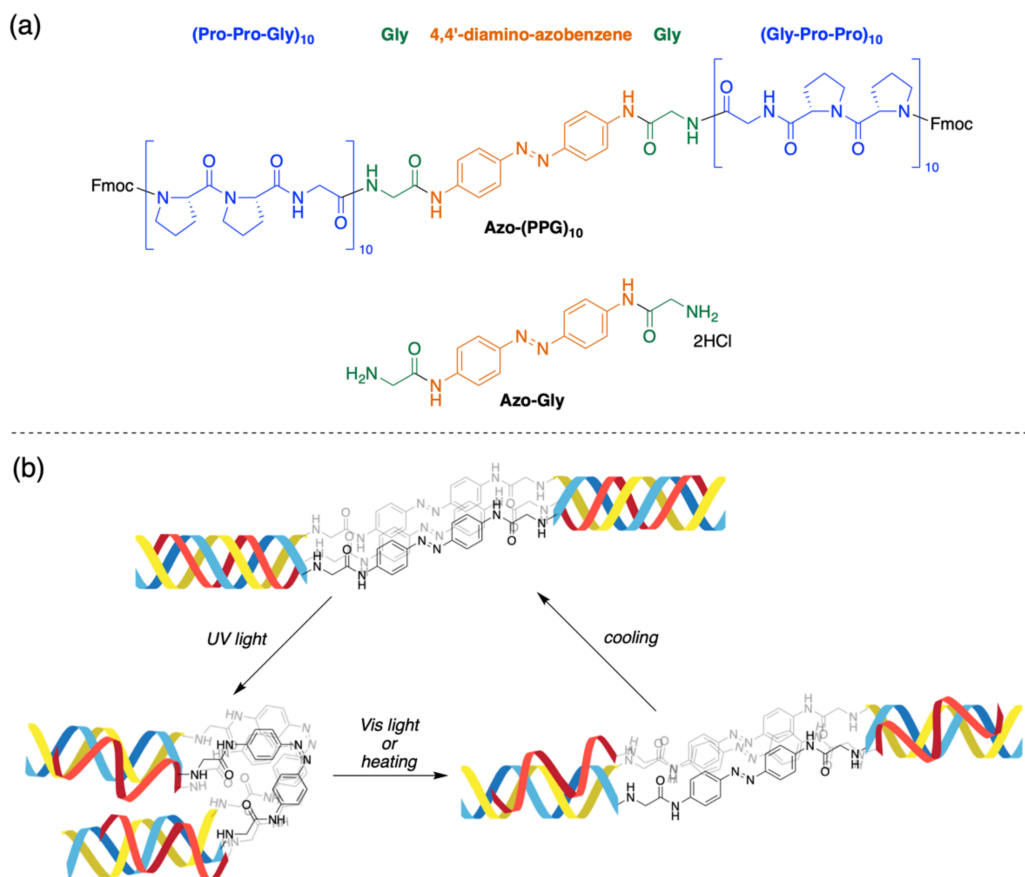


Figure 1. (a) Design of the light-responsive CMP **Azo-(PPG)₁₀** and azobenzene linker unit **Azo-Gly**. (b) Expected mechanism for controlling the triple helical structure of **Azo-(PPG)₁₀**.

2. Materials and Methods

2.1. Synthesis

General. All amino acids, di-*tert*-butyl dicarbonate (Boc₂O), 4-(hydroxymethyl)phenoxy polyethyleneglycol resin (Wang-PEG resin), piperidine, 1-((dimethylamino)(dimethyliminio)methyl)-1*H*-benzo[*d*][1,2,3]triazole 3-oxide hexafluorophosphate (HBTU), 1*H*-benzo[*d*][1,2,3]triazol-1-ol monohydrate (HOBt·H₂O), *N,N*-diisopropylethylamine (DIEA), trifluoroethanol, 2,2,2-trifluoroacetic acid (TFA), and 4 M HCl in 1,4-dioxane were purchased from Watanabe Chemical Industries, Ltd., Hiroshima, Japan. 4,4'-Diaminoazobenzene was obtained from Alfa Aesar, Co., Ltd., Massachusetts, USA. All solvents and other reagents were from FUJIFILM Wako Pure Chemical Co., Ltd., Osaka, Japan. Silica (60- μ m average particle size) was used for column chromatography. Gel filtration chromatography was carried out using Sephadex LH-20 and *N,N*-dimethylformamide (DMF). Electrospray ionization time-of-flight mass spectrometry (ESI-TOF-MS) and fast atom bombardment mass spectrometry (FAB-MS) data were obtained in the positive ion mode and are reported for the protonated molecular ion. The absorbance was measured using a GE Healthcare Ultrospec 3300 pro ultraviolet–visible spectrophotometer or a JASCO V-550 ultraviolet–visible spectrophotometer. Deionized water was obtained from a Milli-Q Plus system (Merck Millipore Co., Ltd., Darmstadt, Germany).

2.1.1. Synthesis of Fmoc-PPG-OH

Synthesis of 2. Boc₂O (7.86 g, 36.0 mmol, 1.2 equiv) was added to a mixture of H-Gly-OH (1, 2.25 g, 30.0 mmol, 1.0 equiv) and Et₃N (6.30 mL, 45.0 mmol, 1.5 equiv) in H₂O (30 mL) and 1,4-dioxane (30 mL) at 0 °C, and the reaction mixture was stirred overnight from 0 °C to room temperature. The reaction mixture was concentrated in vacuo, and the residue was diluted with 4% NaHCO₃ and washed with Et₂O. The aqueous layer was neutralized with citric acid monohydrate, and the desired compound was extracted with EtOAc. The organic layer was washed with brine, dried over anhydrous MgSO₄, and filtered. The filtrate was concentrated in vacuo, and the desired compound was crystallized with petroleum ether, filtered, and dried under reduced pressure to give **2** as a white powder (5.16 g, 29.4 mmol, 98%).

Synthesis of 3. BnBr (4.10 mL, 35.3 mmol, 1.1 equiv) was added to a mixture of **2** (5.16 g, 29.4 mmol, 1.2 equiv) and Et₃N (9.00 mL, 64.8 mmol, 2.2 equiv) in DMF (30 mL) at 0 °C, and the reaction mixture was stirred overnight from 0 °C to room temperature. Additional Et₃N (4.50 mL, 32.4 mmol, 1.1 equiv) and BnBr (2.10 mL, 17.7 mmol, 0.6 equiv) were added, and the reaction mixture was stirred overnight at room temperature. The reaction mixture was concentrated in vacuo, and the residue was diluted with EtOAc. The organic layer was washed with 4% NaHCO₃ and brine, dried over anhydrous MgSO₄, and filtered. The filtrate was concentrated in vacuo, and the desired compound was crystallized with Et₂O and petroleum ether, filtered, and dried under reduced pressure to give **3** as a white powder (4.86 g, 18.2 mmol, 62%).

Synthesis of 4. Compound **3** (5.31 g, 20.0 mmol, 1.0 equiv) was treated with 4 M HCl/1,4-dioxane (60 mL) at room temperature for 2 h. The reaction mixture was concentrated in vacuo, and the desired compound was crystallized with petroleum ether, filtered, and dried under reduced pressure to give **4** as a white powder (4.00 g, 19.8 mmol, 99%).

Synthesis of 6. Boc₂O (7.86 g, 36.0 mmol, 1.2 equiv) was added to a mixture of H-L-Pro-OH (**5**, 3.45 g, 30.0 mmol, 1.0 equiv) and Et₃N (6.30 mL, 45.0 mmol, 1.5 equiv) in H₂O (30 mL) and 1,4-dioxane (30 mL) at 0 °C, and the reaction mixture was stirred overnight from 0 °C to room temperature. The reaction mixture was concentrated in vacuo, and the residue was diluted with 4% NaHCO₃ and washed with Et₂O. The aqueous layer was neutralized with citric acid monohydrate, and extracted with EtOAc. The organic layer was washed with brine, dried over anhydrous MgSO₄, and filtered. The filtrate was concentrated in vacuo, and the desired compound was crystallized with petroleum ether, filtered, and dried under reduced pressure to give **6** as a white powder (6.11 g, 28.5 mmol, 95%).

Synthesis of 7. Et₃N (3.50 mL, 24.0 mmol, 1.2 equiv) was added to a solution of **4** (4.00 g, 19.8 mmol, 1.0 equiv) in DMF (40 mL) at 0 °C, and **6** (5.20 g, 24.0 mmol, 1.2 equiv), *N,N'*-dicyclohexylcarbodiimide (DCC, 4.95 g, 24.0 mmol, 1.2 equiv), and HOBT·H₂O (3.68 g, 24.0 mmol, 1.2 equiv) were added, and the reaction mixture was stirred overnight from 0 °C to room temperature. The reaction mixture was concentrated in vacuo, and the residue was diluted with EtOAc and 10% citric acid and filtered. After separation of the aqueous layer, the organic layer was washed with 10% citric acid, brine, 4% NaHCO₃, and brine, dried over anhydrous MgSO₄, and filtered. The filtrate was concentrated in vacuo, and the resulting yellow oil was purified by column chromatography [silica, CHCl₃/MeOH (99/1)] to give **7** as a white foam (7.91 g, 19.8 mmol, quant.).

Synthesis of 8. Compound **7** (7.91 g, 19.8 mmol, 1.0 equiv) was treated with 4 M HCl/1,4-dioxane (60 mL) at room temperature for 2 h. The reaction mixture was concentrated in vacuo to obtain **8** as a yellow oil (8.00 g, 19.8 mmol, quant.).

Synthesis of 9. Fmoc-OSu (11.1 g, 33.0 mmol, 1.1 equiv) was added to a mixture of H-L-Pro-OH (**5**, 3.45 g, 30.0 mmol, 1.0 equiv) and Na₂CO₃ (15.9 g, 150 mmol, 5.0 equiv) in H₂O (125 mL) and 1,4-dioxane (125 mL) at 0 °C, and the reaction mixture was stirred overnight from 0 °C to room temperature. The reaction mixture was concentrated in vacuo, and the residue was diluted with sat. Na₂CO₃ and washed with Et₂O. The aqueous layer was neutralized with citric acid monohydrate, and the desired compound was extracted

with EtOAc. The organic layer was washed with brine, dried over anhydrous MgSO_4 , and filtered. The filtrate was concentrated in vacuo, and the desired compound was crystallized with ethyl acetate and petroleum ether, filtered, and dried under reduced pressure to give **9** as a white powder (9.53 g, 28.2 mmol, 94%).

Synthesis of 10. DIEA (10.5 mL, 24.0 mmol, 1.2 equiv) was added to a solution of **8** (8.00 g, 19.8 mmol, 1.0 equiv) in DMF (60 mL) at 0 °C, and **9** (8.10 g, 24.0 mmol, 1.2 equiv), HBTU (9.10 g, 24.0 mmol, 1.2 equiv), and HOBT·H₂O (3.68 g, 24.0 mmol, 1.2 equiv) were added, and the reaction mixture was stirred overnight from 0 °C to room temperature. The reaction mixture was concentrated in vacuo, and the residue was diluted with EtOAc. The organic layer was washed with 10% citric acid, brine, 4% NaHCO_3 , and brine, dried over anhydrous MgSO_4 , and filtered. The filtrate was concentrated in vacuo, and the resulting brown oil was purified by column chromatography [silica, $\text{CHCl}_3/\text{MeOH}$ (98/2)] to give **10** as a white foam (9.78 g, 16.6 mmol, 84%).

Synthesis of 11. A suspension of **10** (9.78 g, 16.6 mmol, 1.0 equiv) and 5% Pd/C powder in MeOH (200 mL) was stirred under an H₂ atmosphere at room temperature until the reaction was completed. The reaction mixture was filtered, and the filtrate was concentrated in vacuo. The desired compound was crystallized with petroleum ether, filtered, and dried under reduced pressure to give **11** as a white powder (6.20 g, 14.1 mmol, 85%).

2.1.2. Synthesis of Fmoc-(PPG)₁₀-OH

Synthesis of 13. Wang-PEG resin (**12**, 2.00 g, 0.48 mmol, 1.0 equiv) was swelled with CH_2Cl_2 . To a suspension of the resin in CH_2Cl_2 (15 mL), Fmoc-Gly-OH (0.210 g, 0.74 mmol, 1.5 equiv) and *N,N'*-diisopropylcarbodiimide (DIC, 0.200 mL, 1.40 mmol, 3.0 equiv) were added. After stirring at room temperature for 15 min, 4-dimethylaminopyridine (DMAP, 30.0 mg, 0.24 mmol, 0.5 equiv) was added, and the suspension was stirred overnight at room temperature. After removal of the reaction solution, the resin was washed with CH_2Cl_2 , $\text{CH}_2\text{Cl}_2/\text{EtOH}$ (1/1), EtOH, CH_2Cl_2 , and Et₂O and dried under reduced pressure to give **13** with uncapped OH groups as a yellow resin. Two resin samples (2.00–3.00 mg) were each treated with 20% piperidine/DMF (10 mL) at room temperature for 30 min. According to the absorbance of each reaction solution at 290 nm derived from the Fmoc moiety, the quantity of Fmoc-Gly-OH loaded onto the resin was estimated to be 0.230 mmol/g resin. For capping of the unreacted sites on the resin, Fmoc-Gly-Wang PEG resin was swelled with CH_2Cl_2 . To a suspension of this resin in CH_2Cl_2 (15 mL), was added DIEA (0.240 mL, 1.40 mmol, 3.0 equiv) and Ac₂O (0.130 mL, 1.40 mmol, 3.0 equiv), and the suspension was stirred at room temperature for 2 h. After removal of the reaction solution, the resin was washed with CH_2Cl_2 , DMF, CH_2Cl_2 , and Et₂O and dried under reduced pressure to give acetyl-capped **13** as a yellow resin.

Synthesis of 14. Compound **13** (2.00 g, 0.460 mmol) was swelled with DMF, and was treated with 20% piperidine/DMF (30 mL) at room temperature for 30 min. After removal of the reaction solution, the resin was washed with DMF, *i*-PrOH, and DMF. To a suspension of the resulting H-peptidyl-Wang PEG resin in DMF (15 mL), Fmoc-amino acid (1.40 mmol, 3.0 equiv), HBTU (0.350 g, 0.920 mmol, 2.0 equiv), HOBT·H₂O (0.140 g, 0.920 mmol, 2.0 equiv), and DIEA (0.320 mL, 1.80 mmol, 4.0 equiv) were added, and the suspension was stirred at room temperature for 2 h. After removal of the reaction solution, the resin was washed with DMF, *i*-PrOH, and CH_2Cl_2 . This deprotection and coupling cycle was repeated until the desired peptide sequence was synthesized. The resulting resin was finally washed with Et₂O and dried under reduced pressure to give **14** as a yellow resin.

Synthesis of 15. Compound **14** was swelled with DMF, and was treated with 20% piperidine/DMF (30 mL) at room temperature for 30 min. After removal of the reaction solution, the resin was washed with DMF, *i*-PrOH, and DMF. To a suspension of resulting H-peptidyl-Wang PEG resin in DMF (15 mL), Fmoc-PPG-OH (**11**, 0.560 g, 1.15 mmol, 2.5 equiv), HBTU (0.350 g, 0.920 mmol, 2.0 equiv), HOBT·H₂O (0.140 g, 0.920 mmol, 2.0 equiv), and DIEA (0.320 mL, 1.80 mmol, 4.0 equiv) were added, and the suspension

was stirred at room temperature for 2 h. After removal of the reaction solution, the resin was washed with DMF, *i*-PrOH, and CH₂Cl₂. This deprotection and coupling cycle was repeated until the desired peptide sequence was synthesized. The resulting resin was finally washed with Et₂O and dried under reduced pressure to give **15** as a yellow resin (2.48 g).

Synthesis of 16. Compound **15** (1 g, 0.240 mmol) was treated with TFA (30 mL) at room temperature for 2 h. The suspension was filtered, and the resin was washed with CH₂Cl₂. The filtrate was concentrated in vacuo with a small amount of H₂O, and the partial residue (0.134 g, 50.0 μmol) was purified by gel filtration column chromatography (Sephadex G-25, 25% AcOH) and lyophilized to give **16** as a white powder (60.0 mg, 22.4 μmol, 12% from **13**): FAB-MS obsd 2775, calcd 2775 [M + Na]⁺, M = C₁₃₅H₁₈₂N₃₀O₃₃.

2.1.3. Synthesis of Azo-Gly and Azo-(PPG)₁₀

Synthesis of 18. DCC (45.0 mg, 0.220 mmol, 2.2 equiv) was added to a solution of Boc-Gly-OH (**2**, 38.0 mg, 0.220 mmol, 2.2 equiv) in CH₂Cl₂, and the reaction mixture was stirred at room temperature for 30 min. To the mixture, 4,4'-diaminoazobenzene (**17**, 21.0 mg, 0.100 mmol, 1.0 equiv) was added, and the reaction mixture was stirred overnight at room temperature. The reaction mixture was concentrated in vacuo, and the residue was diluted with EtOAc and 10% citric acid and filtered. After separation of aqueous layer, the organic layer was washed with 10% citric acid, brine, 4% NaHCO₃, and brine, dried over anhydrous MgSO₄, and filtered. The filtrate was concentrated in vacuo, and the desired compound was crystallized with Et₂O and petroleum ether, filtered, and dried under reduced pressure to give **18** as a yellow powder (69.0 mg, 0.100 mmol, quant.): FAB-MS obsd 527, calcd 527 [M + H]⁺, M = C₂₆H₃₄N₆O₆.

Synthesis of Azo-Gly. Compound **18** (20.0 mg, 40.0 μmol, 1.0 equiv) was treated with 4 M HCl/1,4-dioxane (10 mL) at room temperature for 30 min. The reaction mixture was concentrated in vacuo, and the desired compound was crystallized with Et₂O and petroleum ether, filtered, and dried under reduced pressure to give **Azo-Gly** as a yellow powder (12.0 mg, 32.8 μmol, 82%).

Synthesis of Azo-(PPG)₁₀. DIEA (8.00 μL, 40.0 μmol, 4.0 equiv) was added to a solution of **Azo-Gly** (34 mg, 10.0 μmol, 1.0 equiv) in DMF (5 mL) at 0 °C, and Fmoc-(PPG)₁₀-OH (**16**, 8.10 g, 20.0 μmol, 2.0 equiv), HBTU (9.00 mg, 20.0 μmol, 2.0 equiv), and HOBT·H₂O (4.00 mg, 20.0 μmol, 2.0 equiv) were added, and the reaction mixture was stirred overnight from 0 °C to room temperature. Additional HBTU (9.00 mg, 20.0 μmol, 2.0 equiv), HOBT·H₂O (4.00 mg, 20.0 μmol, 2.0 equiv), and DIEA (8.00 μL, 40.0 μmol, 4.0 equiv) were added, and the reaction mixture was further stirred overnight at room temperature. The reaction mixture was concentrated in vacuo, and the residue was purified by gel filtration column chromatography (Sephadex LH-20, DMF) and lyophilized to give **Azo-(PPG)₁₀** as a white solid (10.0 mg, 1.70 μmol, 17%).

2.2. Measurements and Analysis

General. All sample solutions were preincubated overnight at 4 °C to form the triple helix structure. Circular dichroism (CD) spectra were recorded on a J-820 spectropolarimeter (JASCO Co., Ltd., Hachioji, Japan) equipped with a thermostatic cell holder coupled with a thermo supplier EZL-80F (TAITEC Co., Ltd., Koshigaya, Japan) under a N₂ atmosphere. Experiments were performed with a 1-mm quartz cell over 190–300 nm. UV-Vis spectra were acquired using a Ultrospec 3300 pro (GE Healthcare Co., Ltd., Illinois, U.S.) or V-570 UV/VIS/NIR spectrophotometer (JASCO Co., Ltd., Hachioji, Japan) with a 1-cm quartz cell. For photoisomerization, a Handy UV Lamp SLUV-4 at 365 nm, 4 W (AS ONE Co., Ltd., Osaka, Japan) was used for UV irradiation, and Vis light at 436 nm was produced using an Ultrospec 3300 pro (GE Healthcare Co., Ltd., Illinois, U.S.). The temperature of the sample solutions during absorption measurements was controlled using a thermo bath (AGC TECHNO GLASS Co., Ltd., Haibara, Japan).

2.2.1. CD Measurements

Each sample solution for CD spectroscopy was prepared in water to a concentration of 100 μM and measured over 190–300 nm. To estimate the T_m for **Azo-(PPG)₁₀**, the sample solution was adjusted to 100 μM with water. Thermal denaturation was monitored by measuring the change in dichroic intensities at 227 nm as a function of increasing temperature from 4 to 60 °C. The heating rate was 0.2 °C/min⁻¹.

2.2.2. Photo-Induced Denaturation of Collagen Triple Helix

To investigate the light-induced helix denaturation of **Azo-(PPG)₁₀**, a series of sample solutions were prepared in water at a concentration 100 μM and the spectral data over 190–300 nm were obtained. The incubation of the sample solution at room temperature was carried out in the dark for 1 h. UV irradiation for 1 h was executed with a UV lamp in the dark at room temperature. UV-Vis irradiation for 1 h was performed with UV irradiation for 5 min and subsequent irradiation by a UV/Vis spectrophotometer for 5 min, for six cycles. The helix content was calculated from the maximal peak intensities in the CD spectra according to the following formula:

$$\text{Helix content (\%)} = [\theta]/[\theta]_0, \quad (1)$$

where $[\theta]$ is the maximal mean residue molar ellipticity of the sample solution under the corresponding conditions and $[\theta]_0$ is the maximal mean residue molar ellipticity of the intact helix in the sample solution.

2.2.3. Photo- and Thermal-Reversibility of Azobenzene Moiety

Photo-reversibility was investigated using an aqueous solution of **Azo-(PPG)₁₀** (11.1 μM) in water and **Azo-Gly** (11.7 μM) in 5% MeOH/water because it is less soluble in water than **Azo-(PPG)₁₀**. After measuring the first absorbance data, UV irradiation for 1 min was carried out with a UV lamp in the dark, and then the absorbance data were re-measured. Subsequently, the samples were stood for 5 min at room temperature in the dark, and the absorption was measured.

For the kinetic assay of the *cis*-to-*trans* isomerization caused by a thermal effect, an aqueous solution of 50 μM **Azo-(PPG)₁₀** was prepared. In the case of the measurement for **Azo-(PPG)₁₀** at 40 °C, the concentration was adjusted to 11.1 μM . A solution of **Azo-Gly** (10 μM) was prepared in 5% MeOH in water. Each sample solution was incubated in a water bath in the dark and the absorption was chronologically measured. From the first-order reaction, the kinetic constant was calculated according to the absorbance at 364 nm followed by fitting the curve to minimize the error between the measured value and the regression curve equation with the following formula:

$$[\text{cis-form}]_t = [\text{cis-form}]_0 \cdot \exp(-kt), \quad (2)$$

where $[\text{cis-form}]_t$ is the concentration of the *cis*-form according to the absorbance at 364 nm when measured, $[\text{cis-form}]_0$ is the initial concentration of the *cis*-form regarded as the sample concentration, k is the first order rate constant, and t is the measuring time.

The half-life $t_{1/2}$ was calculated using the rate constant k as follows:

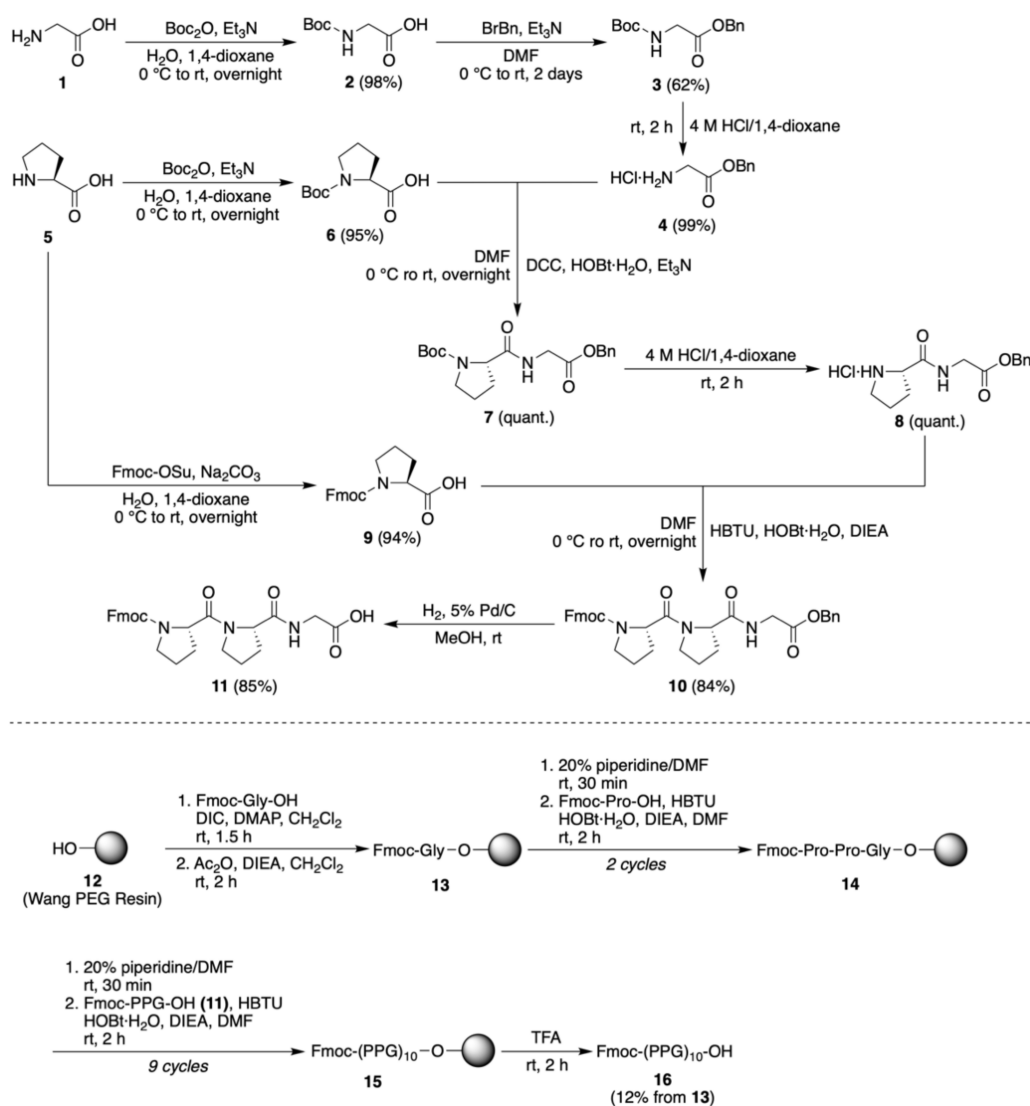
$$t_{1/2} = \ln 2/k = 0.693/k, \quad (3)$$

3. Results and Discussion

3.1. Synthesis of Photo-Responsive CMP

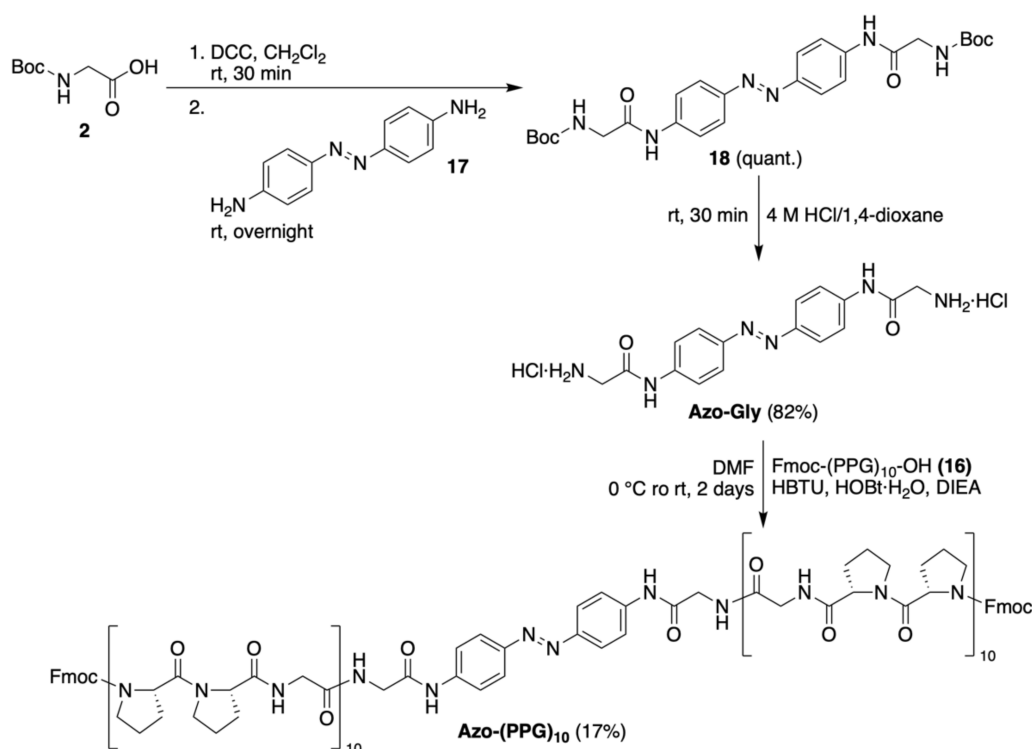
For the synthesis of the CMP **16**, a convergent strategy in which Fmoc-protected Pro-Pro-Gly fragments prepared in solution were coupled to a solid-supported Pro-Pro-Gly fragment was adopted because of the reduced number of couplings required [46]. The component Pro-Pro-Gly tripeptides for the fragment condensation were synthesized by solution-phase methods (Scheme 1). After preparing the Fmoc-Pro-Pro-Gly tripeptide

anchored to the resin via one-by-one peptide chain elongation, Fmoc-(PPG)₁₀-OH was synthesized by fragment condensation with units of Fmoc-PPG-OH **11**.



Scheme 1. Synthesis of Fmoc protected CMP **16**.

For the synthesis of the CMP containing an azobenzene moiety, both amino groups of 4,4'-diaminoazobenzene **17** were reacted with *tert*-butyloxycarbonyl (Boc)-protected glycine **2** (Scheme 2). After deprotecting the Boc groups to provide **Azo-Gly** (Supplementary Figure S1), two molecules of CMP **16** were conjugated to obtain **Azo-(PPG)₁₀**. Although the mass of **Azo-(PPG)₁₀** could not be determined by mass spectrometry techniques, such as fast atom bombardment mass spectrometry, electrospray ionization time-of-flight, or matrix assisted laser desorption/ionization, because of the large molecular weight and intrinsic aggregation property, **Azo-(PPG)₁₀** displayed a characteristic CD curve and the absorption properties of azobenzene, and a single peak was present in liquid-chromatography with a gel permeation column (Supplementary Figure S2). Therefore, we concluded that **Azo-(PPG)₁₀** was successfully synthesized.



Scheme 2. Synthesis of the azobenzene linker **Azo-Gly** and the photo-responsive CMP **Azo-(PPG)₁₀**.

3.2. Investigation of Collagen Triple Helical Properties

The ability of **Azo-(PPG)₁₀** to form a collagen triple helix in water was examined using a CD assay with the positive control, Fmoc-(PPG)₁₀-OH (**16**), to examine the extent of the helix content. The CD spectrum of **Azo-(PPG)₁₀** showed a maximal peak at 227 nm, as was observed for **16**, which indicated that **Azo-(PPG)₁₀** formed a collagen triple helical structure (Figure 2). The slightly lower maximal peak height for **Azo-(PPG)₁₀** compared with **16** was because of the distortion of the collagen terminus caused by the insertion of the azobenzene. However, the peak height of **Azo-(PPG)₁₀** was comparable to that of Fmoc-(PPG)₈-OH (data not shown), which indicated that the triple helical content of **Azo-(PPG)₁₀** was similar to that of Fmoc-(PPG)₈-OH.

The T_m value of **Azo-(PPG)₁₀** was estimated to be approximately 35 °C by monitoring the maximal peak height in the CD spectrum at 227 nm while heating (Figure 3). The T_m value of (Pro-Pro-Gly)₁₀ ranges from 27 to 41 °C, depending on the solvent [47,48], which indicated that **Azo-(PPG)₁₀** has adequate stability toward heating.

3.3. Denaturation of the Collagen Triple Helix Structure by Light Irradiation

Next, the effect of light irradiation on the collagen triple helix was investigated by CD. Incubation of the triple helical solution of **Azo-(PPG)₁₀** at room temperature for 1 h resulted in an 8% decrease in the collagen triple helix content (Figure 4). UV irradiation for 1 h denatured 9% of the helical content. These results indicated that single *trans*-to-*cis* isomerization of the azobenzene moiety did not disrupt the collagen triple helix. In contrast, six cycles of UV-Vis irradiation over 1 h decreased the helical content by 19%, which demonstrated that repetitive isomerization of the azobenzene moiety by UV-Vis irradiation considerably induced the unfolding the triple helix structure of **Azo-(PPG)₁₀**. The completely unfolded **Azo-(PPG)₁₀** could be re-formed to the triple helical structure on cooling. The destabilization, misfolding, or delayed folding of collagen fibers caused by a sequence variant, or mechanical damage of the collagen molecules, is related to several human diseases [49–52]. Although our results indicated that 75% of the helical structure remained, this partial disruption of the structure (i.e., slow unfolding) has the potential

to be used in elucidating the mechanism of the folding/unfolding processes, which may lead to better understanding of diseases related to collagen and the design of treatments for such diseases.

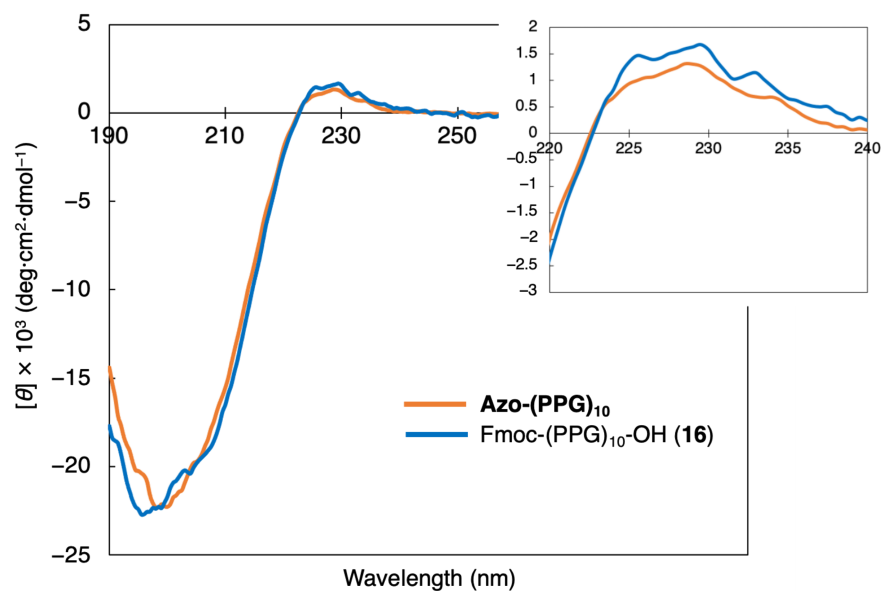


Figure 2. CD spectra of Azo-(PPG)₁₀ and the positive control Fmoc-(PPG)₁₀-OH (16). The inset shows the spectra over the range of the characteristic maximal peak for the collagen triple helix structure.

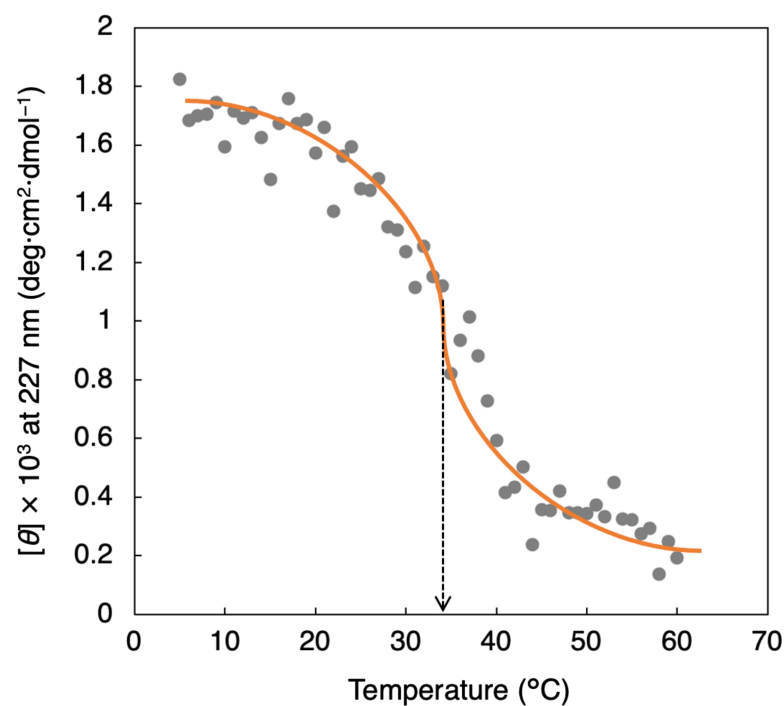


Figure 3. Maximal peak intensity of Azo-(PPG)₁₀ in the CD spectrum at different temperatures.

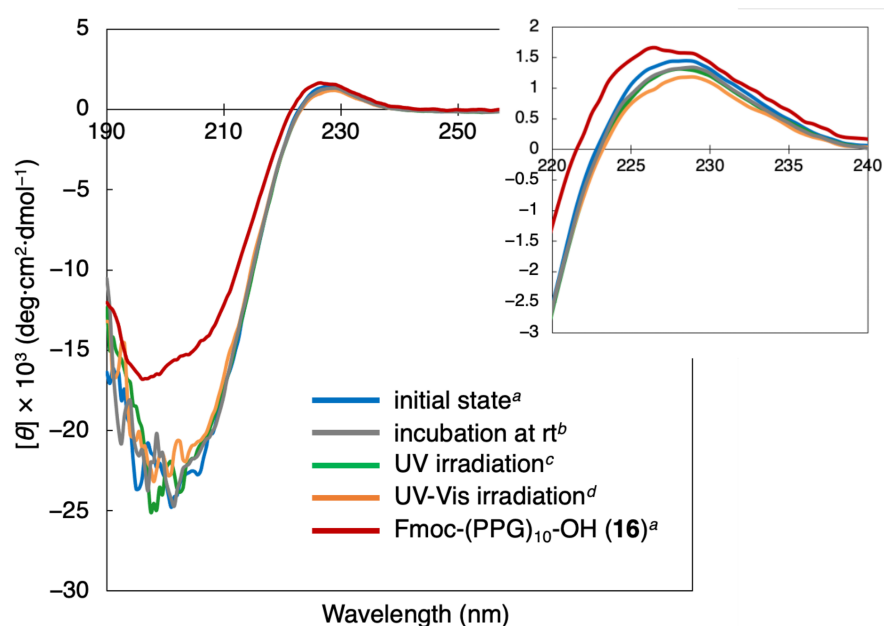


Figure 4. Changes in the CD spectra of **Azo-(PPG)₁₀** upon irradiation with light. ^a Measurement was carried out before light irradiation. ^b Sample solution was incubated at room temperature in the dark, and then measured. ^c The sample solution was continuously irradiated with UV light (365 nm) for 1 h, and then measured. ^d The sample was alternatively irradiated with UV (365 nm, 5 min) and Vis (436 nm, 5 min) light six times, and then measured.

3.4. Isomerization of the Azobenzene Moiety by Light Irradiation or Thermal Effect

To investigate the slow unfolding of **Azo-(PPG)₁₀** upon UV irradiation, and the thermal effect, the isomerization behavior of the internal azobenzene was analyzed. Initially, the reversibility of the *trans*-to-*cis* isomerization upon UV irradiation and the *cis*-to-*trans* isomerization at room temperature (i.e., thermal effect) was evaluated at 20 and 40 °C. The absorption at approximately 350 nm of the *trans*-form of azobenzene is greater than that of the *cis*-form, which enables monitoring of the isomerization of the azobenzene moiety. The azobenzene moiety of **Azo-(PPG)₁₀** at 20 °C showed reversibility of the isomerization, and at 40 °C the reversibility was slightly greater (Figure 5). In comparison with **Azo-Gly**, less reversibility in the conformation of **Azo-(PPG)₁₀** was observed because of the interactions between the CMP chains.

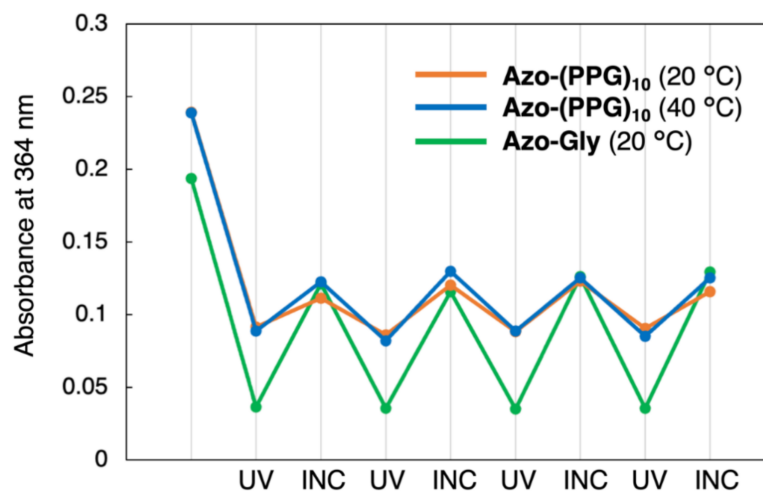


Figure 5. Reversibility of the conformation of the azobenzene moiety at 20 and 40 °C upon UV irradiation (365 nm, 1 min), and incubation at room temperature in the dark (5 min).

In the kinetic assays for the *cis*-to-*trans* isomerization of the azobenzene moiety, changes in the percentage of the *cis*-form were calculated according to the chronological absorption measurements at 364 nm. This isomerization could be considered to be a first-order reaction, and the kinetic constant k and half-life $t_{1/2}$ were calculated by curve fitting (Figure 6).

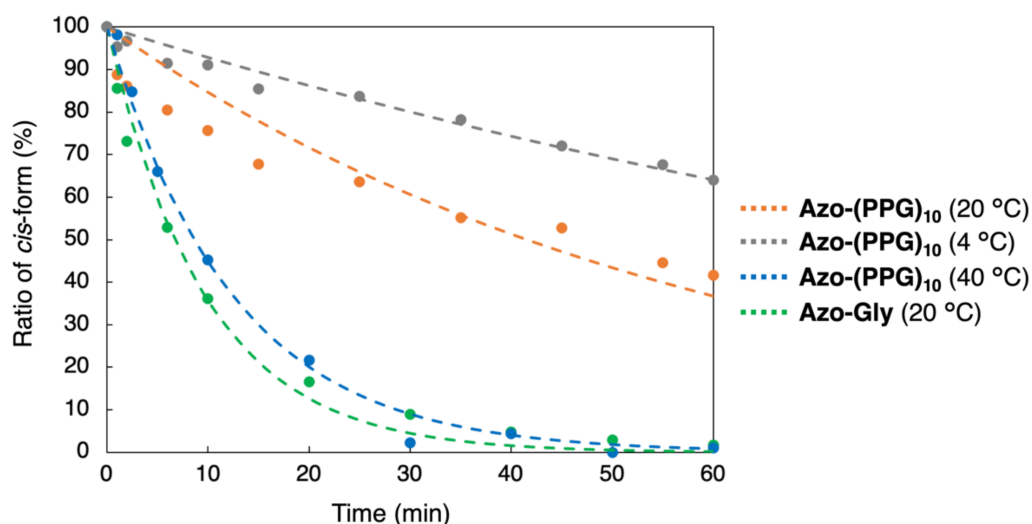


Figure 6. Curve fitting for the *cis*-to-*trans* isomerization of the azobenzene moiety.

The *cis*-to-*trans* recovery rate of the azobenzene moiety in **Azo-(PPG)₁₀** at 20 °C was six-fold slower than that of **Azo-Gly** at same temperature (Table 1). For **Azo-(PPG)₁₀** at 40 °C, the rate was approximately five-fold faster than at 20 °C because of the loose triple helical structure. At a lower temperature (4 °C) compared with 20 °C, the rate of the *cis*-to-*trans* isomerization of **Azo-(PPG)₁₀** was halved. These results are encouraging for the application of **Azo-(PPG)₁₀** not only in investigating the folding/unfolding mechanism of CMPs but also for understanding the behavior of the azobenzene moiety in photo-controllable biomolecules because the kinetics of the CMP folding/unfolding and the isomerization of the azobenzene moiety can be controlled by a combination of light irradiation and heating.

Table 1. Kinetic profile of the isomerization of the azobenzene moiety.

Sample	k (s ⁻¹)	$t_{1/2}$ (min)
Azo-(PPG)₁₀ (20 °C)	1.00	41.6
Azo-(PPG)₁₀ (4 °C)	0.446	93.3
Azo-(PPG)₁₀ (40 °C)	4.82	8.63
Azo-Gly (20 °C)	6.19	6.71

4. Conclusions

In summary, **Azo-(PPG)₁₀** with an azobenzene conjugated at both termini to a (Pro-Pro-Gly)₁₀ chain was successfully designed and synthesized. The light-responsive **Azo-(PPG)₁₀** displayed a collagen triple helix structure with good stability ($T_m = 35$ °C), and this helical structure could be reversibly folded and unfolded depending on the temperature. According to the CD spectral measurements, approximately one-fifth of the triple helical content of **Azo-(PPG)₁₀** was denatured by repetitive UV-Vis irradiation for 1 h. Although the azobenzene moiety in **Azo-(PPG)₁₀** showed reversibility upon UV irradiation and thermal changes, the rate of *cis*-to-*trans* recovery of **Azo-(PPG)₁₀** was relatively slower than that of the azobenzene linker **Azo-Gly** that does not have CMP chains. Higher temperatures induced improvements in the reversibility and kinetic profile of **Azo-(PPG)₁₀** because of the looser helical structure at higher temperatures. The rates of folding/unfolding of the

triple helical structure and isomerization of the azobenzene moiety were adjustable by a combination of light irradiation and heating, indicating that **Azo-(PPG)₁₀** may be useful for developing photo-responsive CMPs and for understanding the assembly/disassembly of CMP chains.

Supplementary Materials: The following supporting information can be downloaded at: <https://www.mdpi.com/article/10.3390/org3040027/s1>, Figure S1: HPLC profile of Fmoc-(PPG)₁₀-OH (**16**); Figure S2: HPLC profile of **Azo-Gly**; Figure S3: GPC profile of **Azo-(PPG)₁₀**.

Author Contributions: Conceptualization, T.K.; validation, D.S., H.G., Y.I. and T.N.; investigation, D.S., H.G., Y.I. and T.N.; writing—original draft preparation, D.S.; writing—review and editing, D.S. and, T.K.; visualization, D.S.; supervision, T.K. All authors have read and agreed to the published version of the manuscript.

Funding: This research received no external funding.

Data Availability Statement: Not applicable.

Conflicts of Interest: The authors declare no conflict of interest.

References

1. Parenteau-Bareil, R.; Gauvin, R.; Berthod, F. Collagen-Based Biomaterials for Tissue Engineering Applications. *Materials* **2010**, *3*, 1863–1887. [[CrossRef](#)]
2. Wang, H. A Review of the Effects of Collagen Treatment in Clinical Studies. *Polymers* **2021**, *13*, 3868. [[CrossRef](#)] [[PubMed](#)]
3. Owczarzy, A.; Kurasiński, R.; Kulig, K.; Rogóż, W.; Szkudlarek, A.; Maciążek-Jurczyk, M. Collagen—Structure, properties and application. *Eng. Biomat.* **2020**, *156*, 17–23. [[CrossRef](#)]
4. Fields, G.B. Synthesis and biological applications of collagen-model triple-helical peptides. *Org. Biomol. Chem.* **2010**, *8*, 1237–1258. [[CrossRef](#)]
5. O’Leary, L.E.R.; Fallas, J.A.; Bakota, E.L.; Kang, M.K.; Hartgerink, J.D. Multi-hierarchical self-assembly of a collagen mimetic peptide from triple helix to nanofibre and hydrogel. *Nat. Chem.* **2011**, *3*, 821–828. [[CrossRef](#)]
6. Ganguly, H.K.; Basu, G. Conformational landscape of substituted prolines. *Biophys. Rev.* **2020**, *12*, 25–39. [[CrossRef](#)]
7. Brodsky, B.; Thiagarajan, G.; Madhan, B.; Kar, K. Triple-helical peptides: An approach to collagen conformation, stability, and self-association. *Biopolymers* **2008**, *89*, 345–353. [[CrossRef](#)]
8. Kubyskhin, V. Stabilization of the triple helix in collagen mimicking peptides. *Org. Biomol. Chem.* **2019**, *17*, 8031–8047. [[CrossRef](#)]
9. Arun, A.; Malrautu, P.; Laha, A.; Luo, H.; Ramakrishna, S. Collagen Nanoparticles in Drug Delivery Systems and Tissue Engineering. *Appl. Sci.* **2021**, *11*, 11369. [[CrossRef](#)]
10. Copes, F.; Pien, N.; Vlierberghe, S.V.; Boccafoschi, F.; Mantovani, D. Collagen-Based Tissue Engineering Strategies for Vascular Medicine. *Front. Bioeng. Biotechnol.* **2019**, *7*, 166. [[CrossRef](#)]
11. Meyer, M. Processing of collagen based biomaterials and the resulting materials properties. *BioMed. Eng. OnLine* **2019**, *18*, 24. [[CrossRef](#)] [[PubMed](#)]
12. Sionkowska, A.; Skrzyński, S.; Śmiechowski, K.; Kołodziejczak, A. The review of versatile application of collagen. *Polym. Adv. Technol.* **2017**, *28*, 4–9. [[CrossRef](#)]
13. Luo, T.; Kiick, K.L. Collagen-like peptides and peptide–polymer conjugates in the design of assembled materials. *Eur. Polym. J.* **2013**, *49*, 2998–3009. [[CrossRef](#)] [[PubMed](#)]
14. Brieke, C.; Rohrbach, F.; Gottschalk, A.; Mayer, G.; Heckel, A. Light-Controlled Tools. *Angew. Chem. Int. Ed.* **2012**, *51*, 8446–8476. [[CrossRef](#)] [[PubMed](#)]
15. Yu, S.M.; Li, Y.; Kim, D. Collagen mimetic peptides: Progress towards functional applications. *Soft Matter* **2011**, *7*, 7927–7938. [[CrossRef](#)]
16. Hamon, F.; Djedaini-Pilard, F.; Barbot, F.; Len, C. Azobenzenes—Synthesis and carbohydrate applications. *Tetrahedron* **2009**, *65*, 10105–10123. [[CrossRef](#)]
17. Pirone, D.; Bandeira, N.A.; Tylkowski, B.; Boswell, E.; Labeque, R.; Valls, R.G.; Giamberini, M. Contrasting Photo-Switching Rates in Azobenzene Derivatives: How the Nature of the Substituent Plays a Role. *Polymers* **2020**, *12*, 1019. [[CrossRef](#)]
18. Hamon, F.; Blaszkiewicz, C.; Buchotte, M.; Banaszak-Léonard, E.; Bricout, H.; Tilloy, S.; Monflier, E.; Cézard, C.; Bouteiller, L.; Len, C.; et al. Synthesis and characterization of a new photoinduced switchable β -cyclodextrin dimer. *Beilstein J. Org. Chem.* **2014**, *10*, 2874–2885. [[CrossRef](#)]
19. Beharry, A.A.; Woolley, G.A. Azobenzene photoswitches for biomolecules. *Chem. Soc. Rev.* **2011**, *40*, 4422–4437. [[CrossRef](#)]
20. Szymański, W.; Beierle, J.M.; Kistemaker, H.A.V.; Velema, W.A.; Feringa, B.L. Reversible Photocontrol of Biological Systems by the Incorporation of Molecular Photoswitches. *Chem. Rev.* **2013**, *113*, 6114–6178. [[CrossRef](#)]
21. Wang, H.; Bisoyi, H.K.; Zhang, X.; Hassan, F.; Li, Q. Visible Light-Driven Molecular Switches and Motors: Recent Developments and Applications. *Chem. Eur. J.* **2022**, *28*, e202103906. [[CrossRef](#)]

22. Lee, I.N.; Dobre, O.; Richards, D.; Ballestrem, C.; Curran, J.M.; Hunt, J.A.; Richardson, S.M.; Swift, J.; Wong, L.S. Photoresponsive Hydrogels with Photoswitchable Mechanical Properties Allow Time-Resolved Analysis of Cellular Responses to Matrix Stiffening. *ACS Appl. Mater. Interfaces* **2018**, *10*, 7765–7776. [[CrossRef](#)] [[PubMed](#)]
23. Siewertsen, R.; Neumann, H.; Buchheim-Stehn, B.; Herges, R.; Nather, C.; Renth, F.; Temps, F.J. Highly Efficient Reversible Z–E Photoisomerization of a Bridged Azobenzene with Visible Light through Resolved S1($n\pi^*$) Absorption Bands. *Am. Chem. Soc.* **2009**, *131*, 15594–15595. [[CrossRef](#)] [[PubMed](#)]
24. Beharry, A.A.; Sadovskii, O.; Woolley, G.A.J. Azobenzene Photoswitching without Ultraviolet Light. *Am. Chem. Soc.* **2011**, *133*, 19684–119687. [[CrossRef](#)]
25. Yang, Y.; Hughes, R.P.; Aprahamian, I.J. Near-Infrared Light Activated Azo-BF₂ Switches. *Am. Chem. Soc.* **2014**, *136*, 13190–13193. [[CrossRef](#)] [[PubMed](#)]
26. Weis, P.; Wu, S. Light-Switchable Azobenzene-Containing Macromolecules: From UV to Near Infrared. *Macromol. Rapid Commun.* **2018**, *39*, 1700220. [[CrossRef](#)]
27. Kumita, J.R.; Smart, O.S.; Woolley, G.A. Photo-control of helix content in a short peptide. *Proc. Natl. Acad. Sci. USA* **2000**, *97*, 3803–3808. [[CrossRef](#)] [[PubMed](#)]
28. Flint, D.G.; Kumita, J.R.; Smart, O.S.; Woolley, G.A. Using an Azobenzene Cross-Linker to Either Increase or Decrease Peptide Helix Content upon Trans-to-Cis Photoisomerization. *Chem. Biol.* **2002**, *9*, 391–397. [[CrossRef](#)]
29. Bredenbeck, J.; Helbing, J.; Kumita, J.R.; Woolley, G.A.; Hamm, P. α -Helix formation in a photoswitchable peptide tracked from picoseconds to microseconds by time-resolved IR spectroscopy. *Proc. Natl. Acad. Sci. USA* **2005**, *102*, 2379–2384. [[CrossRef](#)]
30. Zhang, F.; Sadovskii, O.; Woolley, G.A. Synthesis and Characterization of a Long, Rigid Photoswitchable Cross-Linker for Promoting Peptide and Protein Conformational Change. *ChemBioChem* **2008**, *9*, 2147–2154. [[CrossRef](#)]
31. Samanta, S.; Woolley, A. Bis-Azobenzene Crosslinkers for Photocontrol of Peptide Structure. *ChemBioChem* **2011**, *12*, 1712–1723. [[CrossRef](#)] [[PubMed](#)]
32. Kumita, J.R.; Flint, D.G.; Woolley, G.A.; Smart, O.S. Achieving photo-control of protein conformation and activity: Producing a photo-controlled leucine zipper. *Faraday Discuss.* **2002**, *122*, 89–103. [[CrossRef](#)] [[PubMed](#)]
33. Schrader, T.E.; Cordes, T.; Schreier, W.J.; Koller, F.O.; Dong, S.L.; Moroder, L.; Zinth, W.J. Folding and Unfolding of Light-Triggered β -Hairpin Model Peptides. *Phys. Chem. B* **2011**, *115*, 5219–5226. [[CrossRef](#)] [[PubMed](#)]
34. Spekowius, J.; Pfister, R.; Helbing, J.J. Folding and Unfolding of the Tryptophan Zipper in the Presence of Two Thioamide Substitutions. *Phys. Chem. B* **2021**, *125*, 7662–7670. [[CrossRef](#)]
35. Tochitsky, I.; Banghart, M.R.; Mourrot, A.; Yao, J.Z.; Gaub, B.; Kramer, R.H.; Trauner, D. Optochemical control of genetically engineered neuronal nicotinic acetylcholine receptors. *Nat. Chem.* **2012**, *4*, 105–111. [[CrossRef](#)]
36. Schierling, B.; Noël, A.J.; Wende, W.; Hien, L.T.; Volkov, E.; Kubareva, E.; Oretskaya, T.; Kokkinidis, M.; Römpf, A.; Spengler, B.; et al. Controlling the enzymatic activity of a restriction enzyme by light. *Proc. Natl. Acad. Sci. USA* **2010**, *107*, 1361–1366. [[CrossRef](#)]
37. Fortin, D.L.; Banghart, M.R.; Dunn, T.W.; Borges, K.; Wagenaar, D.A.; Gaudry, Q.; Karakossian, M.H.; Otis, T.S.; Kristan, W.B.; Trauner, D.; et al. Photochemical control of endogenous ion channels and cellular excitability. *Nat. Methods* **2008**, *5*, 331–338. [[CrossRef](#)]
38. Umeki, N.; Yoshizawa, T.; Sugimoto, Y.; Mitsui, T.; Wakabayashi, K.; Maruta, S. Incorporation of an Azobenzene Derivative into the Energy Transducing Site of Skeletal Muscle Myosin Results in Photo-Induced Conformational Changes. *J. Biochem.* **2004**, *136*, 839–846. [[CrossRef](#)]
39. Asanuma, H.; Liang, X.; Nishioka, H.; Matsunaga, D.; Liu, M.; Komiyama, M. Synthesis of azobenzene-tethered DNA for reversible photo-regulation of DNA functions: Hybridization and transcription. *Nat. Prot.* **2007**, *2*, 203–212. [[CrossRef](#)]
40. Kusebauch, U.; Cadamuro, S.A.; Musiol, H.J.; Lenz, M.O.; Wachtveitl, J.; Moroder, L.; Renner, C. Photocontrolled Folding and Unfolding of a Collagen Triple Helix. *Angew. Chem. Int. Ed.* **2006**, *45*, 7015–7018. [[CrossRef](#)]
41. Kusebauch, U.; Cadamuro, S.A.; Musiol, H.J.; Moroder, L.; Renner, C. Photocontrol of the Collagen Triple Helix: Synthesis and Conformational Characterization of Bis-cysteinyll Collagenous Peptides with an Azobenzene Clamp. *Chem. Eur. J.* **2007**, *13*, 2966–2973. [[CrossRef](#)] [[PubMed](#)]
42. Lorenz, L.; Kusebauch, U.; Moroder, L.; Wachtveitl, J. Temperature- and Photocontrolled Unfolding/Folding of a Triple-Helical Azobenzene-Stapled Collagen Peptide Monitored by Infrared Spectroscopy. *ChemPhysChem* **2016**, *17*, 1314–1320. [[CrossRef](#)] [[PubMed](#)]
43. Higashi, N.; Yoshikawa, R.; Koga, T. Photo-responsive azobenzene interactions promote hierarchical self-assembly of collagen triple-helical peptides to various higher-order structures. *RSC Adv.* **2020**, *10*, 15947–15954. [[CrossRef](#)]
44. Koga, T.; Ikejiri, A.; Higashi, N. Narcissistic Self-Sorting of Amphiphilic Collagen-Inspired Peptides in Supramolecular Vesicular Assembly. *Langmuir* **2022**, *38*, 2294–2300. [[CrossRef](#)]
45. Koga, T.; Kingetsu, S.; Higashi, N. Supramolecular Nanofibers from Collagen-Mimetic Peptides Bearing Various Aromatic Groups at N-Termini via Hierarchical Self-Assembly. *Int. J. Mol. Sci.* **2021**, *22*, 4533. [[CrossRef](#)]
46. Ottl, J.; Musiol, H.J.; Moroder, L.J. Heterotrimeric collagen peptides containing functional epitopes. Synthesis of single-stranded collagen type I peptides related to the collagenase cleavage site. *Pept. Sci.* **1999**, *5*, 103–110. [[CrossRef](#)]
47. Xu, Y.; Kirchner, M. Collagen Mimetic Peptides. *Bioengineering* **2021**, *8*, 5. [[CrossRef](#)]
48. Holmgren, S.K.; Bretscher, L.E.; Taylor, K.M.; Raines, R.T. A hyperstable collagen mimic. *Chem. Biol.* **1999**, *6*, 63–70. [[CrossRef](#)]

49. Zitnay, J.L.; Li, Y.; Qin, Z.; San, B.H.; Depalle, B.; Reese, S.P.; Buehler, M.J.; Yu, S.M.; Weiss, J.A. Molecular level detection and localization of mechanical damage in collagen enabled by collagen hybridizing peptides. *Nat. Commun.* **2017**, *8*, 14913. [[CrossRef](#)]
50. Zitnay, J.L.; Jung, G.S.; Lin, A.H.; Qin, Z.; Li, Y.; Yu, S.M.; Buehler, M.J.; Weiss, J.A. Accumulation of collagen molecular unfolding is the mechanism of cyclic fatigue damage and failure in collagenous tissues. *Sci. Adv.* **2020**, *6*, eaba2795. [[CrossRef](#)]
51. Hartmann, J.; Zacharias, M. Mechanism of collagen folding propagation studied by Molecular Dynamics simulations. *PLoS Comput. Biol.* **2021**, *17*, e1009079. [[CrossRef](#)] [[PubMed](#)]
52. Baum, J.; Brodsky, B. Real-time NMR investigations of triple-helix folding and collagen folding diseases. *Fold. Des.* **1997**, *2*, 53–60. [[CrossRef](#)]